JOURNAL OF MATERIALS SCIENCE 13 (1978) 553–562

Analysis of the alternating current properties of ionic conductors

A. K. JONSCHER*
Laboratoire de Chemie du Solide du CNRS, Université de Bordeaux I, 33405 Talence, France

A method of analysis of inclined semicircular complex impedance (Z) diagrams for ionic conductors has been developed on the basis of the concept of "non-Debye" behaviour of solid dielectrics. This approach replaces the rather arbitrary distribution of relaxation times by the physically much simpler concept of a frequency-independent ratio of energy lost per cycle to energy stored. This criterion of dielectric behaviour leads directly to complex admittance (Y) plots in the form of straight lines inclined to the vertical which then transform to inclined semicircles in Z. The use of Y diagrams gives better accuracy of representation and it is shown how this can be further enhanced by plotting $\log Y_i - \log Y_r$ instead of the usual linear representation. Different parts of the graphs are assigned to "bulk" and "barrier" regions on the basis of the value of the dielectric permittivity and it is shown that a hitherto unrecognized physical process can manifest itself as a strong dispersion at frequencies intermediate between the high-frequency bulk response and the low-frequency barrier-dominated behaviour.

1. Introduction

The complex impedance loci of many ionic solids, especially the so-called fast ion conductors, give at sufficiently high frequencies well-defined semicircles passing either through or close to the origin and having their axes depressed below the real axis by an angle $\alpha\pi/2$, Fig. 1. At lower frequencies these semicircles go over into what appears to be the beginning of another semicircle, also inclined to the real axis, although these are usually not sufficiently developed in the available range of frequencies.

The inclined semicircular impedance plots are commonly, if rather loosely "interpreted" in terms of so-called distributions of relaxation times, with the angle α providing a "measure" of the breadth of this distribution [1–3]. This is done, one infers, by analogy with the well-known Cole–Cole construction in the complex permittivity plane in which the experimental results are approximated to by an inclined semicircle, represented by the expression [4]:

$$\epsilon = \epsilon_\infty + \frac{\epsilon_s - \epsilon_\infty}{1 + (i\omega\tau)^{1-\alpha}} \quad (1)$$

where ϵ_∞ and ϵ_s denote, respectively, the high-frequency and static values of ϵ, and τ is a

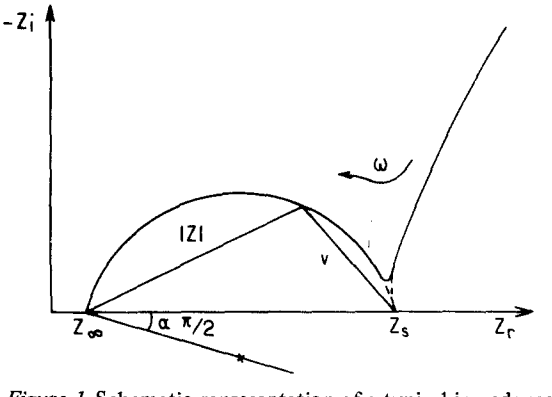

Figure 1 Schematic representation of a typical impedance diagram of an ionic conductor, showing a semicircular arc inclined at an angle $\alpha\pi/2$ and a low-frequency spur which may itself be a circular arc and is also inclined. The significance of the parameter v is defined in the text.

*Permanent address: Chelsea College, University of London, Pulton Place, London, UK.

relaxation time. Equation 1 is said to represent the effect of a distribution of relaxation times and the parameter α is again taken to measure the breadth of this distribution. However, it is not made clear by what process the particular form of Equation 1 is to be derived from a summation of straight semicircles and what physical parameters determine the particular distribution to be employed. In fact, Equation 1 represents nothing more than the mathematical operation of tilting the semicircle through the angle $\alpha\pi/2$ and any physical significance of this operation has yet to be established, as was clearly pointed out in the original paper [4].

It has to be stressed that, despite their geometrical resemblance, inclined semicircles in the ϵ-plane given by Equation 1 and those in the Z-plane given by:

$$Z = Z_r - iZ_i = \frac{Z_s - Z_\infty}{1 + (i\omega\tau)^{1-\alpha}} \quad (2)$$

are in no way equivalent. The definitions of the complex impedance, Z, admittance, Y, and permittivity ϵ being:

$$Y = 1/Z = i\omega\epsilon. \quad (3)$$

It is evident that, while a straight semicircle ($\alpha = 0$) in ϵ transforms into a similar one in Z, tilted semicircles will never transform into one another. It is not possible, therefore, to interpret Equations 1 and 2 in terms of the same physical process.

It is easily shown, with reference to Fig. 1, that the magnitude of the parameter v is given by [5]:

$$v = |Z|(\omega\tau)^{1-\alpha}, \quad (4)$$

and this gives a means of determining the frequency dependence of the impedance. Up to this point no mention has been made of any physical processes coming into play, the entire analysis being purely formal and based on geometrical concepts.

A more specifically physical approach to the interpretation of inclined circular arc impedance diagrams has been developed by Macdonald in an impressive series of papers [6]. Macdonald ascribes the entire frequency dependence of the impedance data to interfacial processes at electrodes and at internal grain boundaries which limit the transparency of these barriers to different ionic species. An extreme case of such limitation is the diffusive boundary giving rise to the classical Warburg impedance. In Macdonald's analysis the bulk ionic conductor has no intrinsic frequency dependence of its own and the fitting of experimental data has to be achieved by postulating suitable sets of barrier parameters, a procedure corresponding closely to the fitting of distributions of relaxation times described previously. As in the former case, it is not easy to judge the physical correctness of this procedure in view of the lack of independent knowledge of the parameters involved. This uncertainty prompts us to present the following altogether different approach to the interpretation of the complex impedance data, in the hope that it may provide a deeper insight into the nature of the physical processes involved.

2. The universal dielectric response

It has been pointed out elsewhere [7] that the tilted impedance semicircles may be more clearly understood in terms of the admittance diagram which must, by definition, represent a straight line inclined at an angle $\alpha\pi/2$ to the vertical, as shown in Fig. 2. This may be considered to represent the admittance diagram of a parallel combination of an ideal, frequency-independent conductance, G_v, and a dispersive, frequency-dependent capacitance, $C_n(\omega)$:

$$Y(\omega) = G_v + i\omega C_n(\omega) \quad (5)$$

with $G_v = (Z_s - Z_\infty)^{-1}$ and C_n given by the relation:

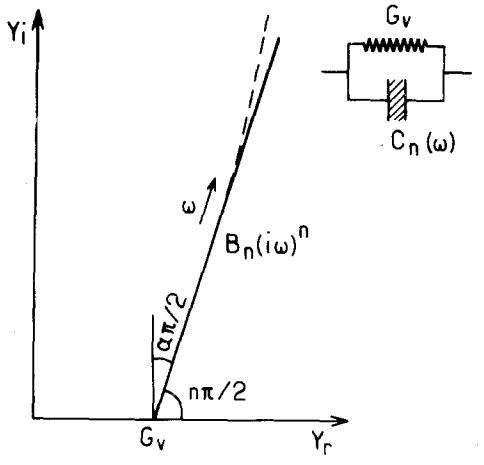

Figure 2 Schematic representation of the admittance $Y = (Z - Z_\infty)^{-1}$, obtained by inverting the high-frequency semicircle in Fig. 1. The effective parallel conductance G_v and "non-Debye" capacitance $C_n(\omega)$ are shown in the equivalent circuit. The dotted line shows a departure from the ideal straight line which is discussed in Section 3.

$$C_n(\omega) = A_n[1 - i\cot(n\pi/2)]\,\omega^{n-1}$$
$$= B_n(i\omega)^{n-1}. \quad (6)$$

Here A_n and $B_n = A_n/\sin(n\pi/2)$ are constants and we have set the exponent

$$n = 1 - \alpha. \quad (7)$$

It may be noted that this definition does not contain τ, the relaxation time, which has no particular physical meaning in the present context.

The point was made [7] that the capacitance C_n which fully accounts for the empirically observed shape of the admittance diagram, has a direct relationship to a physically highly significant phenomenon. It has been shown [8, 9] that the dielectric susceptibility,

$$\chi(\omega) = \epsilon(\omega) - \epsilon_\infty = \chi'(\omega) - i\chi''(\omega), \quad (8)$$

of a very wide range of solids follows, over a wide range of frequencies, the "universal" law

$$\chi(\omega) = a_n[1 - i\cot(n\pi/2)]\,\omega^{n-1}, \quad (9)$$

implying that the ratio

$$\frac{\chi''(\omega)}{\chi'(\omega)} = \frac{\text{energy lost per cycle}}{\text{energy stored per cycle}}$$
$$= \cot(n\pi/2). \quad (10)$$

is independent of frequency. This "non-Debye" behaviour is in sharp contrast with the classical Debye law for which this ratio is equal to $\omega\tau$. It was suggested that the energy ratio of Equation 10 represents a much more significant physical criterion of dielectric behaviour than the arbitrary and rather vague concept of distribution of relaxation times. For a given, empirically determined exponent n, the value of the ratio of Equation 10 is determined uniquely by the universally applicable Kramers–Kronig relations. The physical basis of the observed behaviour is seen in many-body interactions between dipoles or charges which are responsible for the dielectric behaviour of the solid [8].

The observed "universal" dielectric response of solid materials is thus expressed in terms of the frequency dependence of the real and imaginary parts of the complex permittivity:

$$\epsilon'(\omega) = \epsilon_\infty + a_n\omega^{n-1} \quad (11)$$

$$\epsilon''(\omega) = a_n\cot(n\pi/2)\omega^{n-1} \quad (12)$$

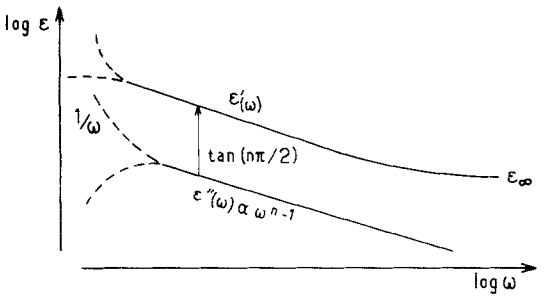

Figure 3 Logarithmic representation of the frequency response of real and imaginary components of the complex dielectric permittivity for a "non-Debye" dielectric, showing the frequency dependence as ω^{n-1} for ϵ'' and $\epsilon' - \epsilon_\infty$. The low-frequency behaviour of ϵ'' may show either a loss peak or a steep rise due to d.c. conductivity or to other anomalies. The real part ϵ' would correspondingly show a saturation or a $1/\omega$ rise.

where the constant a_n is related to B_n in Equation 6 by:

$$B_n = C_0 a_n = (\epsilon_0 S/w)a_n \quad (13)$$

with C_0 denoting the geometrical capacitance of the sample, ϵ_0 the permittivity of free space, S the electrode area and w the sample thickness. The dependence of ϵ' and ϵ'' on frequency is shown schematically in Fig. 3. In general, the low-frequency part of ϵ'' may show one of two types of departure from the ideal graph – either a loss peak [10] or a rise proportional to $1/\omega$ due to the direct current conductivity σ_0. In our procedure, the latter is removed by the subtraction of the conductance G_v from the real part of Y, as will be described later. The presence of a loss peak is seldom evident in experimental results for fast ion conductors.

Any given material may show the presence of two or more parallel mechanisms of the type given by Equations 11 and 12, with the attendant loss peaks. The resultant permittivity is then given by the sum of the individual contributions by the separate physical mechanisms responsible for dielectric polarization in the medium. The fundamental difference between the present approach and the accepted "Debye–Cole–Cole" philosophy, however, is that the latter requires a distribution of mechanisms, with suitable relaxation times, to explain every behaviour departing from the ideal Debye shape, while the present approach interprets a typically observed "flat" frequency dependence by a *single* mechanism,

with one parameter n relating to a wide range of frequencies by means of the energy criterion which is a direct consequence of Kramers-Kronig relations.

The form of Y given by Equations 5 and 6 is now seen as the limiting case applicable when ϵ_∞ is negligible in Equation 11. The existence of good circular arc Z-plots confirms that this is usually a good approximation in a wide range of frequencies. A more detailed analysis of cases where ϵ_∞ is not negligible will be given below.

3. Numerical analysis of high-frequency data

We begin by inverting the Z-plot semicircles, using appropriate values for Z_∞, if different from zero. This gives an inclined straight line in the admittance plot, or at least should do so if the high-frequency impedance was correctly represented by a circular arc. This completely determines the parameters G_v and $C_n(\omega)$. If the experimental points lie sufficiently close to a straight line, the slope of this line is equal to $\tan(n\pi/2)$ and therefore determines the exponent n in Equation 6. It is now instructive to carry out a check of the accuracy and consistency of the data by fitting the corresponding frequency dependence to the admittance, which should follow the relation given by Equations 5 and 6:

$$Y(\omega) = Y_r + iY_i = G_v + B_n(i\omega)^n. \quad (14)$$

If the fit of the frequency points is satisfactory then the interpretation is self-consistent. Depending upon the quality and reliability of the available experimental data, complications may arise in their numerical evaluation resulting in failure to obtain self-consistent results.

One obvious source of error is the presence of a finite lead inductance, L, in series with the specimen. This results in departures from the ideal circular arc at the high-frequency end of the Z-plot, as shown schematically in Fig. 4, and may even lead to a change of sign of Z_i. Since these departures are equal to ωL, it may be possible to correct the results if a circular arc can be found such that each experimental point can be brought on to it by raising vertically by the amount ωL. This recovers the true sample impedance and extends the available range of frequencies for which inversion into the Y-plane can now be made. A similar type of distortion may arise as a result of the presence of a finite stray capacitance

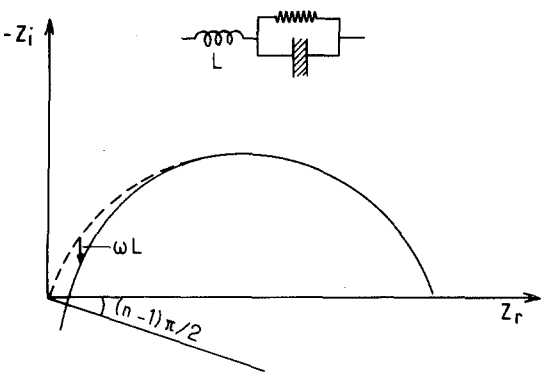

Figure 4 The distortion of the true bulk impedance response by a stray inductance L in series with the sample. It may be possible to reconstruct the semicircle by suitable fitting of vertical corrections equal to ωL.

across the measuring resistor which is used to calibrate the unknown impedance of the sample.

There may be other departures from the ideal behaviour and these become much more pronounced in the Y representation than on the conventional Z-plots, mainly owing to the fact that the eye is much more sensitive to departures from a straight line than from a circular arc. Conversely, the fitting of a straight line is much more positive than that of a circular arc which leaves a lot of scope to imagination, as may be ascertained by examining some of the published data. This is one of the advantages of the admittance plots.

Another commonly found difficulty is that linear plotting of Y_i against Y_r results in a wide separation of points in the upper range of the frequency scale, especially if the measurements are taken on a logarithmic frequency scale. This makes it difficult to see the results in their entirety and the recommended technique is to plot the data in a $\log Y_i - \log Y_r$ representation [11]. This immediately reveals any inconsistencies between the high- and the low-frequency ends of the spectrum. In evaluating the logarithmic plots it is well to bear in mind that a linear relationship $Y_i = bY_r$ becomes, in the logarithmic representation, a straight line of slope 1 but raised by the *factor b* above the line $Y_i = Y_r$, as shown in Fig. 5. In the presence of an offset on the linear graph, $Y_i = b(Y_r - G_v)$, the logarithmic representation shows a rapid drop towards G_v which is then easily corrected.

The principal form of high-frequency departure from the ideal relationship of Equation 14, which

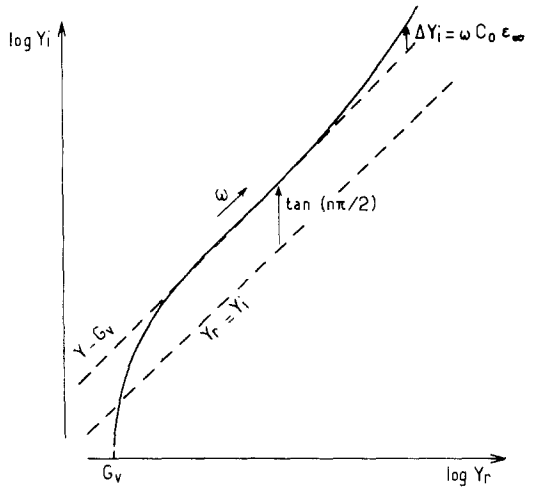

Figure 5 The logarithmic representation of the complex admittance diagram corresponding to the linear representation shown in Fig. 2. A much wider range of frequencies can now be accommodated making it easier to evaluate the consistency of the frequency dependence and the value of the parameter ϵ_∞.

becomes clear in the logarithmic representation, is a steady rise of the experimental plot above the ideal line, as shown in Fig. 5. This may be due to the increasing importance of the term ϵ_∞ in Equation 11 against the diminishing contribution of $\chi'(\omega)$. The contribution of ϵ_∞ gives rise to a difference between the measured values and the extrapolated ideal values from Equation 14.

$$\Delta Y_i = \omega C_0 \epsilon_\infty. \tag{15}$$

A fitting of this difference to the experimental data leads directly to the value ϵ_∞.

4. Effect of electrode resistance

Most dielectric samples used for impedance measurements have some form of evaporated or otherwise applied metallic electrodes which may be relatively thin, say, of the order of 1 μm or less. With samples of high conductance and capacitance this may lead to effects which are not negligible and which may affect the shape of the characteristics, giving a false impression of the properties of the material in question.

The effective equivalent circuit is a distributed line and the detailed analysis is complicated, involving Bessel functions of a complex argument which will not be given here. However, in the limit of an infinitely large *linear* (rather than the more usual circular) geometry, this effect leads to the expression identical to the Warburg impedance, i.e. a semicircle depressed by an angle $\pi/4$. A distributed line is an exact representation of the Warburg diffusive inertia model.

5. Determination of "volume" permittivity

Having obtained an admittance diagram which had been duly corrected for stray inductance effects and which, apart from the ϵ_∞ rise at high frequencies, shows a well-defined value of G_v and of n, it is now possible to claim that this plot represents the properties of a homogeneous region of the sample. The conductance G_v represents here all physical processes giving rise to steady state transport of charge from one electrode to the other. The "non-Debye" capacitance $C_n(\omega)$ represents the purely dielectric effects present in the medium. Since we are dealing with a homogeneous medium which will be presumed to be the volume of the sample, apart from any thin barrier layers in series, it is now permissible to convert to dielectric permittivity characterizing this medium. In this way we obtain for the relative permittivity:

$$\epsilon'(\omega) = \frac{Y_i}{\omega C_0} \tag{16}$$

and loss

$$\epsilon''(\omega) = \frac{Y_r - G_v}{\omega C_0} \tag{17}$$

and these may be plotted against frequency in the manner of Fig. 3 and used in a physical interpretation of the behaviour of the material – a detailed discussion of this aspect of the analysis will be the subject of a separate paper.

The main justification for the identification of the ϵ parameters so determined with the bulk or volume properties is based on the order of magnitude obtained for the relative permittivity ϵ'. Depending on the physico-chemical nature of the material, values of ϵ' in the range 20 to 100 would be considered eminently reasonable for the bulk permittivity. Values in the range 10^3 to 10^5 have been reported and it is tempting to explain them in terms of barrier effects but a more detailed analysis may be required in specific cases.

5. Abnormally "high" values of volume permittivity

It may happen that the low-frequency behaviour of ϵ' shows a steep rise toward lower frequencies, approaching a $1/\omega$ dependence. This is not compatible with any simple circuit artefact, nor is

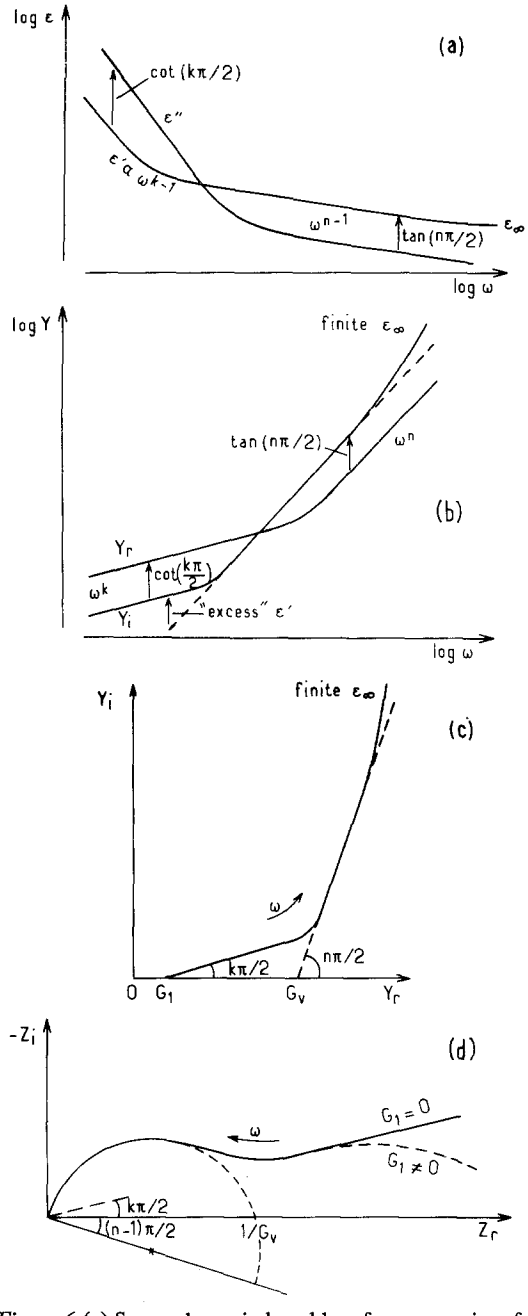

Figure 6 (a) Space-charge induced low-frequency rise of ϵ' and ϵ'', with a "non-Debye" dependence as ω^{k-1}, where $k \sim 0.1$ to 0.2.; (b) The corresponding frequency dependence of the real and imaginary components of Y. The low-frequency behaviour is now "almost" independent of frequency and yet does not constitute d.c, (c) The complex admittance plot corresponding to (a) and (b). The conductance G_v would have been deduced from experimental data if the low-frequency part were not discovered. The intercept G_1 may be difficult to determine reliably, (d) The effect of the low-frequency space charge anomaly on the impedance diagram. The normal inclined semicircle may be severely distorted, making it impossible to fit a semicircle into the experimental data. The effect of a finite G_1 is also shown.

there at present an accepted physical interpretation for it. It is sufficient to state here that this type of behaviour is observed in different materials at sufficiently low frequencies and it may be associated with space charge effects arising at the electrodes. It is therefore not part of the genuine volume behaviour, but unlike the barrier capacitive effect, it cannot be readily disengaged from the volume properties, which should saturate at a finite value of $\epsilon(0)$ at sufficiently low frequencies. The effect of this steep rise of ϵ' at low frequencies on the admittance and impedance diagrams is easily seen with reference to Fig. 6. Diagram (a) represents schematically the $\log \epsilon - \log \omega$ plots showing two regions, the high-frequency "non-Debye" region with the familiar dependence as ω^{n-1}, n being in the region 0.6 to 0.8 for typical ionic materials. The ϵ' and ϵ'' graphs are parallel and separated by the factor $\tan(n\pi/2)$, implying that for $n > \frac{1}{2}$ the real part is higher than the imaginary. The onset of ϵ_∞ is indicated at high frequencies. At the lower frequencies, the "dispersive law" ω^{k-1} is indicated, with $k \ll 1$, say, typically [11] in the range 0.1 to 0.2. The relative positions of ϵ' and ϵ'' are now reversed, the materials is very "lossy", with $\tan\delta \gg 1$.

Converting these data into the real and imaginary parts of the admittance we get the diagram of Fig. 6b in which at low frequencies the real and imaginary parts show a slow variation with frequency. This is in sharp contrast with, on the one hand, the properties of a classical conductor, for which $Y_r = G_v$ is a constant and Y_i is zero, and on the other hand, the behaviour of the more familiar "non-Debye" capacitor which is represented by the steeper lines in the higher frequency region. The real part depending on ω^k now represents a "not-quite-constant" conductance, a slowly varying or "creeping" d.c.

We now construct the complex admittance diagram, Fig. 6c shown here in linear coordinates. This consists of two straight line portions, with the respective inclinations $k\pi/2$ and $n\pi/2$. The low-frequency line may define a finite intercept G_1, indicating the presence of a true d.c. mechanism, although the experimental evidence for this may be difficult to determine with certainty – very low frequency measurements may be required for this purpose.

We complete our analysis by inverting into the Z-plane. The high-frequency behaviour becomes a

tilted semicircle with the angle of tilt equal to $(n-1)\pi/2$, but the effect of the low-frequency behaviour is to give a shallow "spur" to the diagram which is inclined at an angle $k\pi/2$. We note that this spur influences the high-frequency semicircle over an appreciable range of frequencies, distorting its shape and converting it into a much flatter arc and making it very difficult to fit a circular arc to the results, with the consequent uncertainty as to the value of G_0. The effect of a finite G_1 would be to distort the straight line into a very flat circular arc.

The distortion of Z shown in Fig. 6d would arise from the anomalous rise of ϵ at low frequencies. As we have pointed out, this is a widely observed if little understood phenomenon which we attribute to the onset of space charge in the material. The physical significance of the high values of ϵ' may be easily seen by recalling the definition of the polarization as the dipole moment per unit volume,

$$P = \sum_{\alpha} x_\alpha q_\alpha, \qquad (18)$$

where α denumerates all charged particles in the system, q represents the respective charges and x the displacements under an applied electric field. If we note that a "typical" molecular displacement – of an electron cloud with respect to the nucleus, or of two neighbouring ions with respect to one another – in a field of 10^6 V m^{-1} may be of the order 10^{-4} nm, it is easily seen that a few interatomic jumps involving several atomic displacements (typically 1 nm) may contribute very considerably to the increase of the polarization and hence of the apparent ϵ'.

The effect described here is therefore not a true bulk molecular process; it depends upon transport of charges in the system and on the presence of incompletely transparent or replenishing electrodes. The natural limit of this process is the formation of a fully developed space charge barrier of the Schottky type but this may take a few decades of frequency.

It is equally possible, however, that his strong low-frequency dispersion may arise from the same type of mechanism as that responsible for the more usual "universal response" given by Equation 9 but with a peculiarly low value of the exponent n. In our "screened-hopping" model [8] this may be due to heavy screening of the jumping charges, a situation eminently compatible with a high density of hopping charge carriers to be expected in ionic conductors. This strictly volume process has nothing to do with interfacial phenomena and should give completely linear response. A detailed discussion of these phenomena will form the subject of a separate publication.

It is important, in any given physical situation, to distinguish this phenomenon from the effect of the presence of barrier phenomena, to be discussed in Section 7 and evidenced by the appearance of a sharp minimum in the impedance diagram of Fig. 1. As a general rule it may be stated that the effect of the barrier will reflect itself in an upward swing of the apparent capacitance in the volume region for frequencies up to ten times the frequency of the minimum in the Z plot. If significant departures of the type shown in Fig. 6a are seen, say, at two decades above the minimum frequency, then there exists a reasonable presumption that one is dealing with the type of behaviour discussed in the present section.

6. The effect of the presence of a loss peak

We saw that the effect of a steeply rising loss at low frequencies is to distort the Y-diagram in the manner shown in Fig. 6c. There are many materials, however, in which this effect is not seen, for example because there are good replenishing electrodes, and instead one may find a decrease of ϵ'' at low frequencies, giving rise to a loss peak as shown in Fig. 3. It is easily seen that the effect of the presence of a loss peak on the Y-diagram would be to distort it in the opposite sense, the experimental points following a more nearly vertical line to the right of the inclined line and defining a higher value of G_v.

7. The appearance of barrier phenomena

We now return to the discussion of the "classical" Z-diagram as represented in Fig. 1, showing at low frequencies a "spur" which may be either a straight line inclined to the vertical or a similarly inclined circular arc. The complete circle is seldom revealed in the available frequency ranges.

The existence of a well-defined "spur" region in the Z-plot is clearly identified with a series element in the equivalent circuit of the sample. Provided the spur is well separated in frequency from the main semicircle, an inversion into the admittance plane is possible, taking a suitable value of $Z_s = 1/G_v$. The latter would have been determined previously from the volume analysis

with reasonable accuracy, provided the low-frequency ϵ anomaly does not interfere. The new "spur" admittance:

$$Y = (Z - 1/G_v)^{-1} = G_b + B'_n(i\omega)^{n'} \quad (19)$$

defines a value n' of the exponent and a conductance G_b, in complete analogy with Equation 14 relating to the bulk behaviour. The numerical values of B'_n and G_b indicate a much higher capacitance and lower conductance for this part of the characteristic than were obtained for the bulk. It is therefore reasonable to identify this part with a barrier region in series with the bulk of the sample, having geometrical dimensions smaller by factors of 10^3 to 10^6 than the volume, on the only possible assumption that the absolute value of the permittivity is of the same order as for the volume. The corresponding conductance is now very much lower due to the depletion of available free carriers – ions or electrons – from the barrier region.

The barrier effect is therefore clearly an interfacial phenomenon, but whether it arises at the electrodes or at internal barriers resulting from the presence of grain boundaries, e.g. in a fritted ceramic sample, cannot be determined with certanty from a.c. data alone. If the sample may be presumed to be uniform, e.g. a single crystal or a glassy material without clear phase separation in the glassy matrix, then electrode effects appear very plausible. Here a simple test may consist in the variation of the a.c. amplitude or in the application of a d.c. bias. Barrier phenomena are inherently non-linear and it is to be expected that once the voltage *per barrier* exceeds significantly the thermal voltage kT/e, k being Boltzmann's constant and T the absolute temperature, non-linearity will show in the values of Z. A dramatic representation of this was shown for a chalcogenide glass [11] where the barrier collapsed completely with increasing voltage. Now if in the measurements on a particular sample an a.c. amplitude of, say, 0.1 to 1 volt does not produce any variation of the barrier parameters on the Z diagram, then these cannot be due to a pair of barriers at the electrodes, which would have been very non-linear in this range of voltages. The implication must be that there are many barriers in the system, distributed at internal grain boundaries or other inhomogeneities in such a way that the actual voltage appearing across each barrier is much less than kT/e leaving it safely in the linear region.

The existence of external or internal barriers is inseparable from discontinuities in the flow of charges in the system. In the case of ionic conductors this is a particularly sensitive point, since the provision of suitable replenishing, i.e. non-blocking electrodes is a relatively much more difficult task than in the case of electronic semiconductors. A study of barrier phenomena is therefore a valuable means of obtaining information about the nature of the electrode behaviour and about the suitability of various electrode materials for particular ionic conductors. This emphasizes the importance of extending the measurements sufficiently far into the low frequency region which represents the main source of experimental information at our disposal.

We should note that experimental evidence points clearly to the "non-Debye" nature of the barrier capacitance, although the value of n' may differ somewhat from the bulk n. The conservation of the "non-Debye" property under conditions where carriers are evidently absent clearly points to the existence of separate physical processes respectively giving rise to the d.c. conduction and to the polarization in these ionic materials. This must constitute an important element in any attempt at physical interpretation of the processes governing transport in ionic conductors.

It may appear surprising, at first sight, that a system consisting of a distribution of internal barriers should show the "non-Debye" behaviour, as distinct from the classical Maxwell–Wagner response normally associated with this type of system. There is good experimental evidence to suggest that this is not always the case, materials which are *par excellence* granular in nature, such as dry and humid sand, showing clearly non-Debye behaviour with all the features shown in Fig. 6 [12].

It is worth pointing out that the clear separation into bulk and barrier responses as postulated in the present section may be seriously distorted by the "creeping d.c." effects described in the previous section. This may lead to a Z diagram of the type shown in Fig. 7 which defines three separate regions: the true volume behaviour at high frequencies (i), the low frequency barrier phenomena (ii), and the intermediate region (iii) arising from the ϵ-anomaly. While superficial

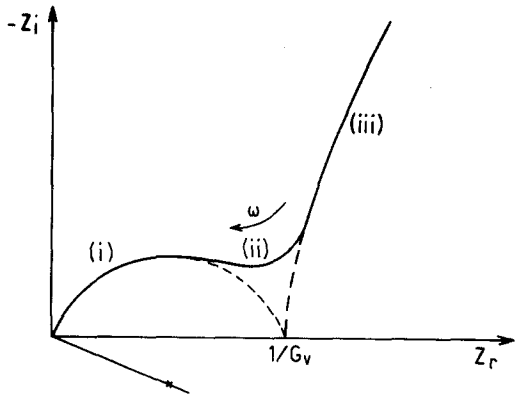

Figure 7 The distortion of a simple "volume–barrier" impedance plot, as shown in Fig. 1, resulting from the presence of a low-frequency anomaly in the ϵ' behaviour, due to the incipient space charge formation. The volume region (i) as now separated from the barrier region (iii) by the intermediate region (ii) which may completely distort the shape of the circular arc.

analysis might regard regions (i) and (ii) as belonging to the bulk behaviour and might therefore derive abnormally high values for the bulk permittivity, a more detailed analysis as outlined in the present paper will avoid this difficulty, by recognizing the separate nature of region (ii).

It may happen that this experiment gives a well-behaved impedance plot of the type shown in Fig. 1, with clear evidence of a volume and a barrier region, but an analysis of ϵ data suggests values of $\epsilon' = 10^4 \epsilon_0$, or even higher. In such cases there may be a strong presumption that one is not dealing with genuine bulk behaviour, but it is important to be cautious in reaching such conclusions. Clearly, if measurements can be made at sufficiently high frequencies, it should be possible to reach the "true" bulk behaviour. However, this is not always possible and another way out may be the measurement at sufficiently low temperatures which may confirm the high values of permittivity as genuine bulk values. This point will be discussed in a separate publication.

We have shown in an early section how the presence of a $1/\omega$ dependence of the permittivity $\epsilon'(\omega)$ may influence the shape of the impedance plot in the low-frequency region. The question arises to what extent might the presence of this $1/\omega$ anomaly be the result of the proximity of the barrier circle, when we evaluate the experimental data in the region of the "dip" between the two arcs in Fig. 1. In this region we may assume that $B_n \omega^n \ll G_v$ so that the impedance may be expressed in the approximate form:

$$Z = (1/G_0)\,[1 - (B_n/G_v)\,(i\omega)^n] + (1/B_n')(i\omega)^{n'}.$$

Assuming for simplicity that the two exponents for the bulk and barrier regions are the same, $n = n'$, we obtain the following approximate expression for the real component of the apparent permittivity in the frequency region corresponding to the transition between the barrier and bulk responses:

$$\epsilon'(\omega) = a_n \epsilon^{n-1} + G_v^2/a_n' \omega^{n+1} \qquad (20)$$

The first term of this is just the contribution of the volume permittivity, while the second term shows a frequency dependence of the type ω^{-n-1}, which is much steeper than $1/\omega$. There should therefore be no risk of confusion between this phenomenon and the anomalous $1/\omega$ dependence described earlier.

8. Conclusions

We have shown how the concept of "non-Debye" response of solid dielectrics, based on an almost universal behaviour of a very wide range of materials, may be applied to the analysis of the impedance diagrams for ionic conductors. A number of complicating features often found in experimental results, such as the effects of stray inductances, electrode resistance, as well as more subtle departures from ideal behaviour are discussed in detail. It is shown that the admittance diagram represents a much more sensitive tool for the interpretation of data and that it reveals important features which may go unnoticed on the impedance plots.

In accepting the "non-Debye" interpretation we move away from the conventional analysis in terms of distributions of Debye-like parameters, which is arbitrary and cannot be substantiated by independently obtained evidence. We are also departing from the alternative widely accepted approach ascribing the shape of the Z-diagram entirely to transmission characteristics of interfacial barriers which, while plausible in itself, cannot be considered to be proved to be correct. Instead we are able to show that the experimental results indicate definite common features between the behaviour of ionic conductors and that of

other dielectrics, features which we ascribe to many-body interactions resulting in partial screening of dipoles and of charges present in the system [8]. This will give us valuable clues with regard to the nature of the transport processes in these solids.

We are able to separate d.c. conduction processes involving continuous transport from one electrode to the other, from distinctly a.c. or dielectric effects which show certain well-defined characteristics. The appearance of anomalously high values of permittivity is explained in terms of a phenomenon of "incipient" space charge formation, which precedes the development of a full barrier. Alternatively, it may arise from certain peculiarities of the screening of charge carriers, resulting in particularly low values of the exponent n in the "universal" response law. Either gives rise in the impedance diagram to a slow transition between the bulk semicircle and the barrier spur, resulting in a significant flattening of the impedance plot which makes it difficult to "fit" semicircles into the data.

Our immediate physical conclusions with regard to the nature of the transport mechanisms in fast ionic conductors may be stated as follows. The "non-Debye" nature of both bulk and barrier characteristics suggests that the conducting species moving by discontinuous jumps interact with one another in a manner demanded by the "screened hopping" mechanism of the "non-Debye" analysis [8]. This contradicts the concept of "free ion" conduction proposed by Rice and Roth [13] but is compatible with a model of "cooperative" hopping" recently proposed by Wang *et al* [14]. A more detailed study of experimental data for a wide range of three- , two- and one-dimensional ionic conductors, which all show essentially similar "non-Debye" behaviour, should help to develop further the theoretical model and provide a better insight into the nature of transport processes in ionic conductors.

Acknowledgement

This work was performed during a period of leave as Visiting Professor at the Université de Bordeaux I, and the author is grateful to Professor P. Hagenmuller for his hospitality and to Dr J. -M. Réau and his colleagues for many useful discussions and for making available numerical data of their measurements.

References

1. J. F. BAUERLE, *J. Phys. Chem.* **30** (1969) 2657.
2. J. -M. RÉAU, J. CLAVERIE, G. CAMPET, C. DEPORTES, D. RAVAINE, J. -L. SOUQUET and A. HAMMON, CR Acad. Sci. (Paris) **280** (1975) 325.
3. T. A. ROTH, *J. Appl. Phys.* **42** (1971) 246.
4. K. S. COLE and R. H. COLE, *J. Chem. Phys.* 9 (1941) 341.
5. D. RAVAINE and J. -L. SOUQUET, CR Acad. Sci. (Paris) **277** Series C, (1973) 489.
6. J. ROSS MACDONALD, "Electrode Processes in Solid State Ionics", edited by M. Kleitz and J. Dupuy, (D. Reidel Dordrecht, 1976) p.149.
7. A. K. JONSCHER, *Phys. Stat. Sol* (a) **32** (1975) 665.
8. *Idem, Nature* **253** (1975) 717.
9. *Idem, Colloid and Polymer Sci.* **253** (1973) 231.
10. *Idem, Nature* **256** (1975) 566.
11. A. K. JONSCHER and M. S. FROST, *Thin Solid Films* **37** (1976) 267.
12. M. SHAHIDI, J. B. HASTED and A. K. JONSCHER, *Nature* **258** (1975) 595.
13. M. J. RICE and W. L. ROTH, *J. Solid State Chemistry* 4 (1972) 294.
14. J. C. WANG, M. GAFFARI and SANG-IL CHOI, *J. Chemical Phys.* **63** (1975) 772.

Received 12 May and accepted 17 June 1977.